

Copper(I)-catalyzed asymmetric 1,3-dipolar cycloaddition of 1,3-enynes and azomethine ylides

Received: 5 January 2022

Accepted: 25 July 2023

Published online: 04 August 2023

Check for updates

Bo-Ran Wang^{1,2}, Yan-Bo Li², Qi Zhang², Dingding Gao¹, Ping Tian¹, Qinghua Li¹ & Liang Yin^{1,2}

Herein, we report a copper(I)-catalyzed asymmetric 1,3-dipolar cycloaddition of azomethine ylides and 1,3-enynes, which provides a series of chiral poly-substituted pyrrolidines in high regio-, diastereo-, and enantioselectivities. Both 4-aryl-1,3-enynes and 4-silyl-1,3-enynes serve as suitable dipolarophiles while 4-alkyl-1,3-enynes are inert. Moreover, the method is successfully applied in the construction of both tetrasubstituted stereogenic carbon centers and chiral spiro pyrrolidines. The DFT calculations are also conducted, which imply a concerted mechanism rather than a stepwise mechanism. Finally, various transformations started from the pyrrolidine bearing a triethylsilylethynyl group and centered on the alkyne group are achieved, which compensates for the inertness of 4-alkyl-1,3-enynes in the present reaction.

Chiral poly-substituted pyrrolidines are not only key structure units in both natural and man-made bioactive molecules but also versatile intermediates in organic synthesis^{1–10}. One of the most efficient methods to access these compounds is the transition metal-catalyzed asymmetric 1,3-dipolar cycloaddition^{11–18}. Among various metal catalysts, copper(I) catalysts have gained a prominent position, which exhibited admirable abilities to enable high reaction efficiency and wonderful asymmetric induction^{19–34}. Various 1,3-dipoles, such as nitrones, azomethine ylides, and azomethine imines, serve as wonderful substrates. The dipolarophiles are generally limited to strongly activated alkenes, including α,β -unsaturated compounds and $\alpha,\beta,\gamma,\delta$ -unsaturated compounds³⁵ (Fig. 1a). The strong electron-withdrawing groups include aldehyde, ketone, ester, amide, cyano, nitro, sulfone, and phosphonate. However, catalytic asymmetric 1,3-dipolar cycloadditions with weakly activated alkenes are very uncommon and thus remain elusive^{36–41}.

In 2016, Cossío, Adrio, and Carretero reported a copper(I)- or silver(I)-catalyzed asymmetric 1,3-dipolar cycloaddition of azomethine ylides and weakly activated alkenes (Fig. 1b, left). In this reaction, vinylarenes bearing electron-deficient aryl groups, as well as vinylheteroarenes, were used as satisfactory 1,3-dipoles³⁶. In 2021, Chung,

Wang, and co-workers successfully developed a copper(I)-catalyzed asymmetric 1,3-dipolar cycloaddition of β -substituted alkenyl heteroarenes by using a powerful chiral monodentate phosphoramidite ligand (Fig. 1b, right)³⁸. Other notable examples are copper-catalyzed asymmetric 1,3-dipolar cycloadditions of fullerenes and cyclopropanes with azomethine ylides^{39–43}. The highly strained nature of the olefin unit in fullerenes enabled the reaction. Despite these leading achievements, the scope of weakly activated alkenes is still significantly limited. Moreover, it is noted that the products in these reactions are structurally specific, which does not allow facile further transformations based on the electron-deficient aryls or heteroaryl. Thus research efforts on the reaction with weakly activated alkenes that are easily functionalized at a later stage are highly desirable^{11–18}.

1,3-Enynes were initially used as important intermediates in the synthesis of highly substituted aromatic rings^{44,45}. Then Krische pioneered the transition metal-catalyzed three-component coupling reactions with 1,3-enynes^{46–55}. In 2004, Krische and co-workers uncovered a rhodium-catalyzed reductive coupling of 1,3-enynes and α -keto aldehydes under a hydrogenation atmosphere, which afforded (*E*)-2-hydroxy-3,5-dien-1-one products⁴⁶. In 2008, the same group disclosed a ruthenium-catalyzed reductive coupling of 1,3-enynes and

¹The Research Center of Chiral Drugs, Shanghai Frontiers Science Center of TCM Chemical Biology, Innovation Research Institute of Traditional Chinese Medicine, Shanghai University of Traditional Chinese Medicine, 1200 Cailun Road, Shanghai 201203, China. ²CAS Key Laboratory of Synthetic Chemistry of Natural Substances, Center for Excellence in Molecular Synthesis, Shanghai Institute of Organic Chemistry, University of Chinese Academy of Sciences, Chinese Academy of Sciences, 345 Lingling Road, Shanghai 200032, China. ✉e-mail: tianping@shutcm.edu.cn; qinghuali@shutcm.edu.cn; liangyin@sioc.ac.cn

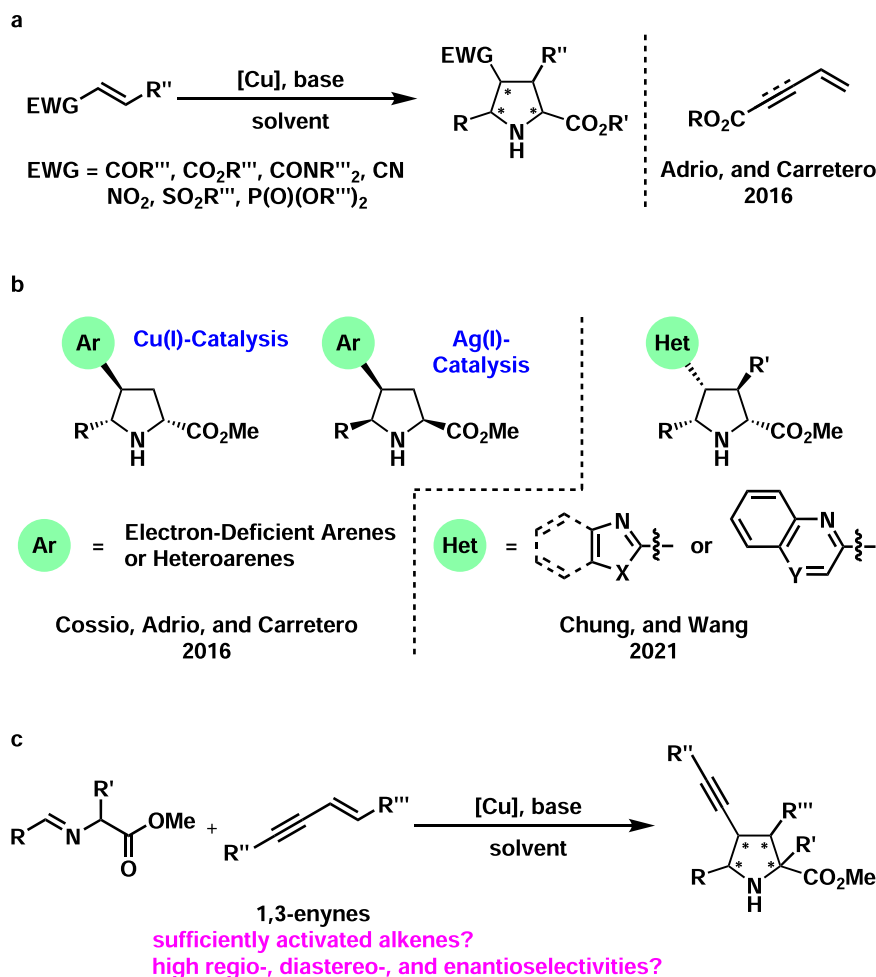


Fig. 1 | Introduction to catalytic asymmetric 1,3-dipolar cycloadditions and our working hypothesis. **a** Classical catalytic asymmetric 1,3-dipolar cycloaddition of α,β -unsaturated and $\alpha,\beta,\gamma,\delta$ -unsaturated compounds. **b** Catalytic asymmetric 1,3-

dipolar cycloaddition of electron-deficient vinylarenes and alkenyl heteroarenes. **c** Catalytic asymmetric 1,3-dipolar cycloaddition of 1,3-enynes: this work.

alcohols, providing synthetically versatile homopropargyl alcohols⁵². These instructive works stimulated further extensive investigations on the utilization of 1,3-enynes in three-component coupling reactions and other interesting transformations^{56–58}, especially copper-catalyzed asymmetric syntheses of propargyl alcohols/amines^{59–63} and allenes^{64–73}. Based on these seminar reports, it is envisioned that the presence of a conjugated carbon-carbon triple bond may lead to weak activation of the olefin group and thus may lower the LUMO energy (Fig. 1c). Thus, 1,3-enynes may serve as potential efficient dipolarophiles. Moreover, the presence of a carbon-carbon triple bond would allow further facile functionalization of the pyrrolidines produced via 1,3-dipolar cycloadditions.

Herein, we would like to disclose a copper(I)-catalyzed asymmetric 1,3-dipolar cycloaddition of azomethine ylides and 1,3-enynes. A series of chiral poly-substituted pyrrolidines were prepared in moderate to high yields with moderate to high diastereo- and enantioselectivities. Remarkably, 1,4-disubstituted 1,3-enynes also served as a suitable dipolarophile. Furthermore, the present methodology worked efficiently in the construction of both tetrasubstituted stereogenic carbon centers and chiral spiro pyrrolidines. The chemical calculations indicated that a concerted reaction pathway rather than a step-wise one was more reasonable for the present reaction. Moreover, the activation ability of the terminal olefin by several substituents was studied, which gave us a clear understanding of the reactivities of these weakly activated terminal olefins. At last, multiple transformations

showcased the synthetic versatility of the triethylsilylethynyl group and thus complemented the substrate shortage of 4-alkyl-1,3-enynes.

Results and discussion

Initially, the reaction between iminoester **1a** and 1,3-enyne **2a** was investigated for the optimization of reaction conditions (Fig. 2). In the presence of 5 mol% Cu(CH₃CN)₄PF₆, 6 mol% (*R*)-Tol-BINAP, and 20 mol% KO^tBu, **3aa** was produced in 44% yield with 10/1 dr and 29% ee (entry 1). Several bisphosphines and (*R,R*)-*t*Bu-FOXAP were screened (entries 2–7), which identified (*R*)-DTBM-SEGPHOS as the best in terms of yield, dr, and ee (entry 7, 72% yield, >20/1 dr, 80% ee). Switching the solvent from THF to toluene led to increased enantioselectivity but with decreased both yield and dr (entry 8, 45% yield, 16/1 dr, 97% ee). DCM was found to be the most suitable solvent as **3aa** was obtained in 72% yield with >20/1 dr and 98% ee (entry 9). Barton's base worked with similar efficiency (entry 10). However, weaker organic bases, such as Et₃N and Cy₂NMe, were found to be ineffective. The reaction with Cs₂CO₃ as the base afforded **3aa** in excellent yield together with excellent diastereo- and enantioselectivities (entry 11, 96% yield, >20/1 dr, 98% ee). The yield was further enhanced in DCE by increasing the substrate concentration from 0.1 to 0.4 M (entry 12, 99% yield, >20/1 dr, 98% ee). The reaction results of both 'butyl and benzyl esters (**1a'** and **1a''**) were also satisfactory (entry 13, 99% yield, >20/1 dr, 96% ee; entry 14, 98% yield, >20/1 dr, 98% ee). It should be noted that only one type of regioisomers was observed in these reactions.

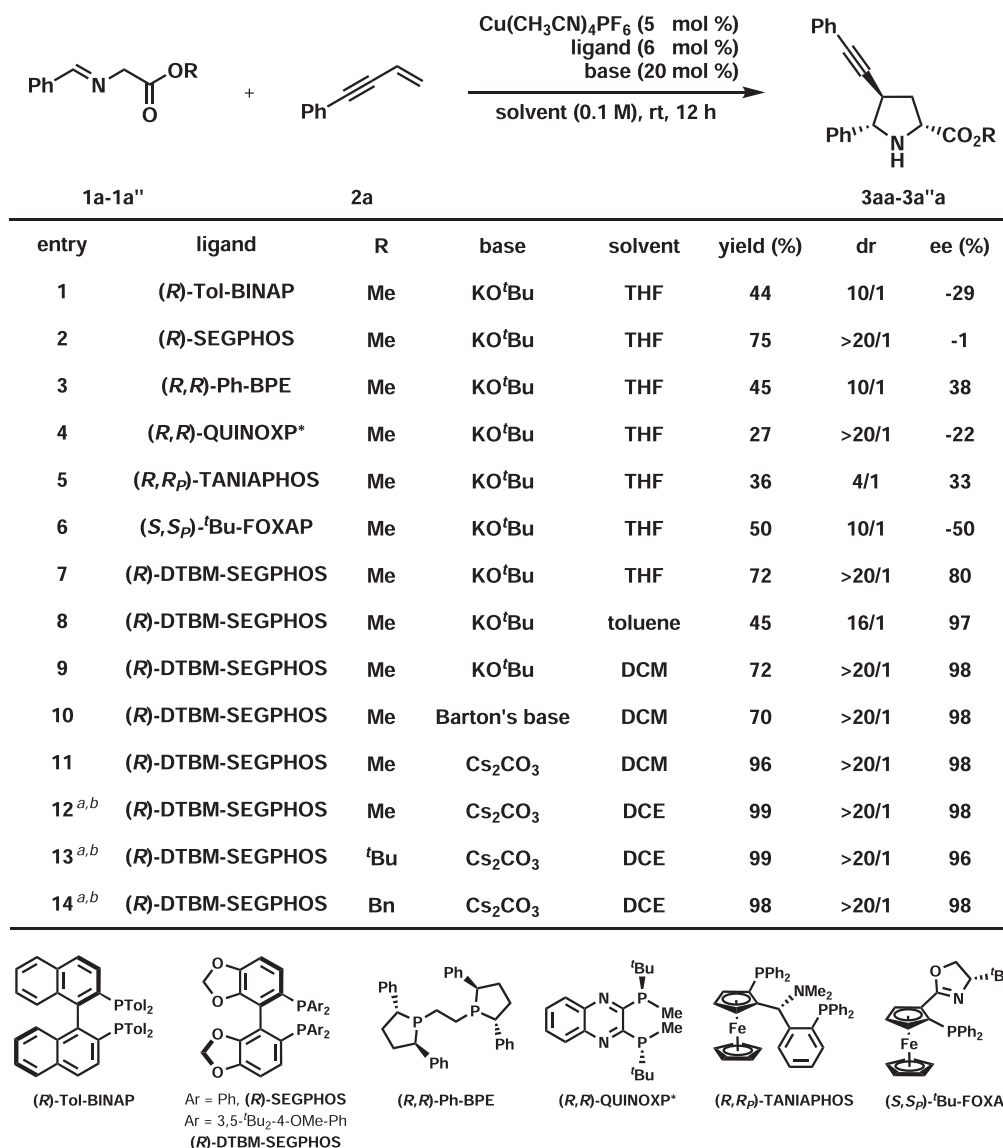


Fig. 2 | Optimization of reaction conditions. Reaction conditions: **1a-1a''** (0.13 mmol), **2a** (0.10 mmol). Yields were determined by ¹H NMR analysis of the reaction crude mixture using CH₂Br₂ as an internal standard. Ee and dr were

determined by chiral-stationary-phase HPLC analysis. THF = tetrahydrofuran, DCM = dichloromethane, DCE = ClCH₂CH₂Cl. Barton's base = 2-^tbutyl-1,1,3,3-tetramethylguanidine. ^a0.4 M. ^bIsolated yield.

Under the optimum reaction conditions, the substrate scope of iminoester (**1**) was studied with **2a** as the dipolarophile (Fig. 3). The reaction results were not very sensitive to both the substitution pattern and the electronic nature of the aryl groups as the corresponding products were isolated in generally high yields with excellent diastereo- and enantioselectivities (**3ba-3ja**, 72–99%, 14/1–20/1 dr, 95–98% ee). However, moderate dr (14/1) was observed in the case of **3ca** and moderate yield (72%) was obtained in the reaction of **3ia**. Moreover, 1-naphthyl and 2-naphthyl were well accepted (**3ka-3la**, 95–96%, >20/1 dr, 94% ee). Heteroaryl substituents were also well tolerated, and the corresponding products were obtained with excellent results (**3ma-3oa**, 94–98%, >20/1 dr, 91–97% ee). As for the aliphatic iminoesters (**1p-1s**), (*S,S_p*)-^tBu-FOXAP was found as a better ligand than (*R*)-DTBM-SEGPPOS. Under higher substrate concentration (1.0 M), several aliphatic iminoesters reacted with **2a** smoothly to provide the corresponding products in acceptable results (**3pa-3sa** and **3ri**, 57–73%, 9/1–12/1 dr, 79–90% ee). However, the results of aliphatic iminoesters were inferior to the results of aromatic ones. The absolute configuration of **3ri** was determined by X-ray analysis of its derivative's single

crystals (for the details, see SI), which led to the assignment of the configurations of **3pa-3sa**.

Then the substrate scope of 1,3-enynes (**2**) was investigated with **1a** as the 1,3-dipole precursor (Fig. 4). At first, 1,3-enynes bearing a terminal olefin were evaluated (R' = H). The R group could be various aromatic substituents (**3ab-3am**, 80–99%, 13/1–20/1 dr, 93–99% ee). Clearly, both the substitution pattern and the electronic nature of the aryl groups did not have a significant effect on yield, diastereo-, or enantioselectivities. However, the electron-donating group led to slightly decreased both yield and diastereoselectivity (**3ad**, 80%, 13/1 dr). Heteroaromatic substituents were well accepted in the R group (**3an-3ao**, 78–97%, >20/1 dr, 98–99% ee). When the R group was an aliphatic substituent (such as PhCH₂CH₂-), the reaction did not proceed at all. Fortunately, the R group could be either an additional alkynyl group or an *N*-Bn-sulfamide, and the products were isolated with satisfying results (**3ap-3aq**, 80–96%, >20/1 dr, 98–99% ee). Furthermore, 1,3-enyne **2r** containing a triethylsilyl group served as a satisfactory 1,3-dipolarophile, which was transformed to **3ar** in 80% yield with >20/1 dr and 99% ee. Evidently, the synthetically versatile triethylsilyl group allows facile

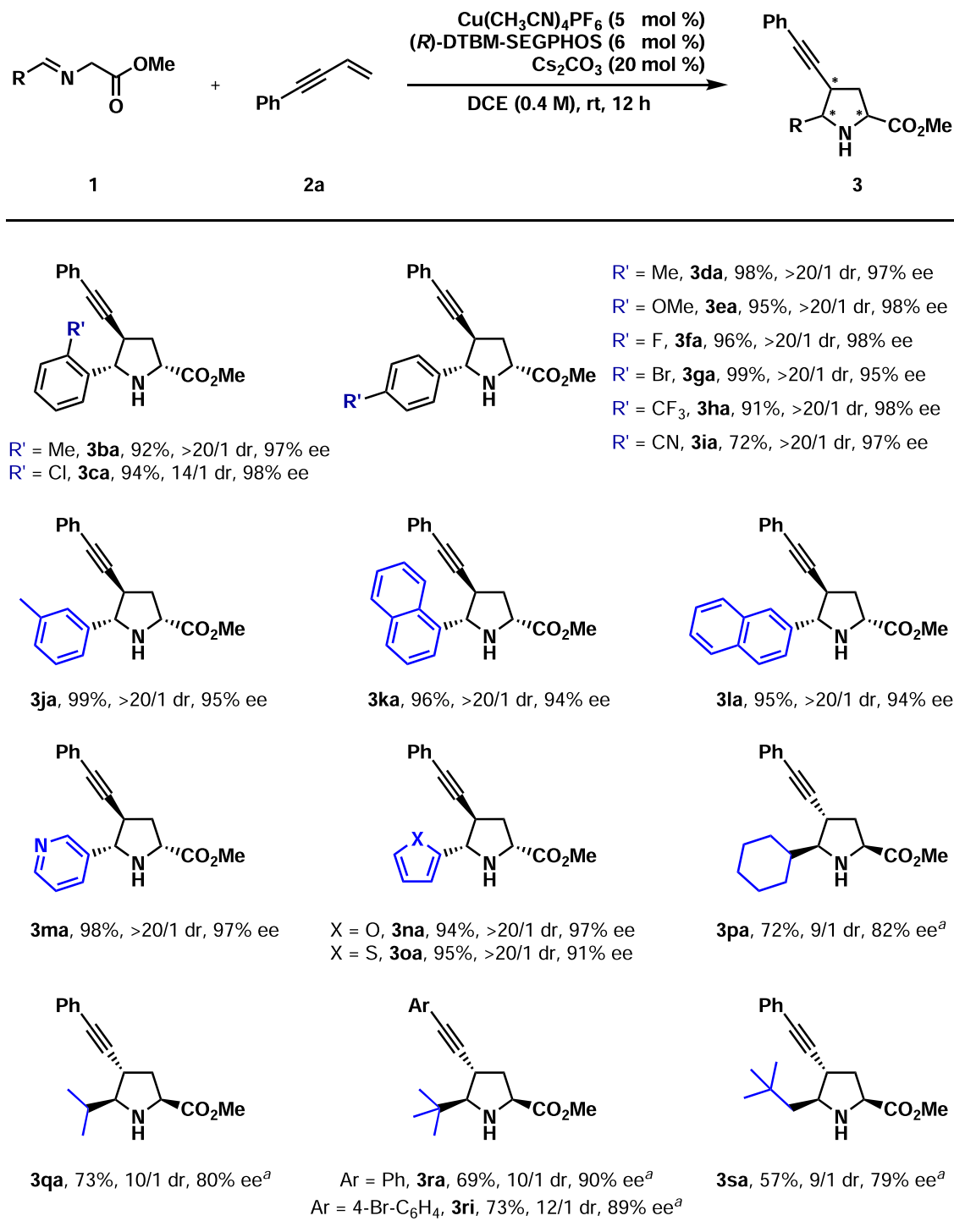


Fig. 3 | Substrate scope of azomethine ylides 1. Reaction conditions: **1** (0.26 mmol), **2a** (0.20 mmol). Isolated yields were reported. Ee and dr were determined by chiral-stationary-phase HPLC analysis. ^a(S,S_p)-^tBu-FOXAP was used instead of (R)-DTBM-SEGPPOS in DCE (1.0 M). 18 h.

late-stage functionalization. Then *trans*-1,4-disubstituted 1,3-enyne **2s** (R = Ph, R' = Me) was tried in the present reaction. Although the yield was moderate in the reaction with 10 mol% copper(I) catalyst and 40 mol% Cs₂CO₃, both the diastereo-, and enantioselectivities were very high (**3as**, 49%, >20/1 dr, 92% ee). Interestingly, *cis*-1,3-enyne **2t** (R = Ph, R' = Me) exhibited similar performances in the present catalytic system (**3at**, 54%, >20/1 dr, 98% ee). It should be noted that **3as** and **3at** are diastereoisomers. The absolute configuration of **3ai** was determined unambiguously by X-ray crystal diffraction. The stereochemistry of other products (**3aa–3oa** and **3ab–3at**) was deduced by

structural analogy. It should be pointed out that the relative configuration of **3as** was further confirmed by the X-ray analysis of its single crystals.

Subsequently, the present method was applied in the construction of tetrasubstituted stereocenters (Fig. 5). By introducing a methyl group at the α -position in the iminoester, substrate **4** was obtained for this purpose. The reactions of **4** and several 1,3-enynes proceeded nicely with excellent diastereo- and high enantioselectivities (**6a**, **6d**, **6j**, **6n**, and **6r**, >20/1 dr, 78–92% ee). However, yields varied considerably (28–99%). At 60 °C, as low as 28% yield was

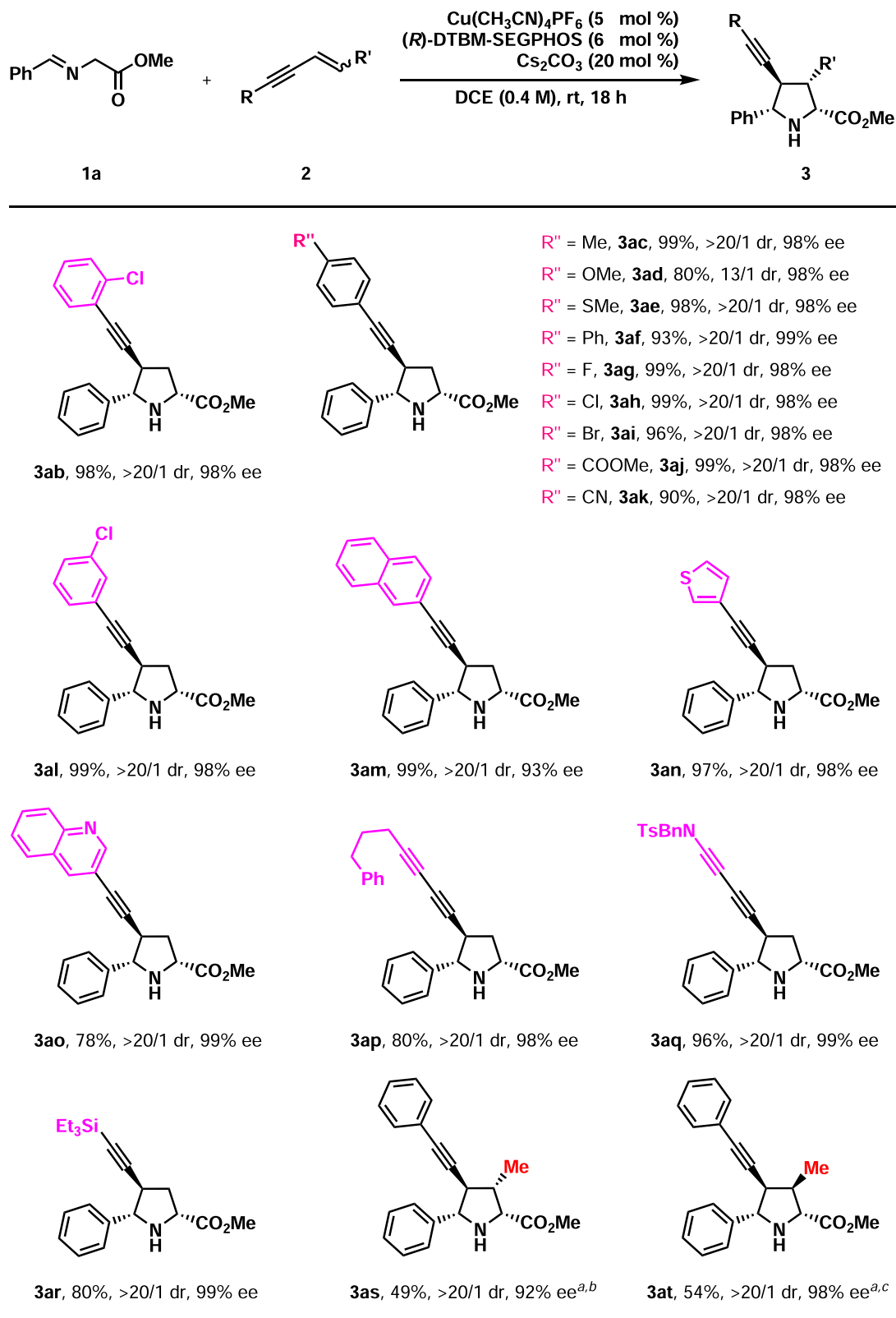


Fig. 4 | Substrate scope of 1,3-enynes 2. Reaction conditions: **1a** (0.26 mmol), **2** (0.20 mmol). Isolated yields were reported. Ee and dr were determined by chiral-stationary-phase HPLC analysis. ^a10 mol% catalyst and 40 mol% Cs₂CO₃ were used. 1.0 M. 48 h. ^b*trans*-1,3-enyne used. ^c*cis*-1,3-enyne used.

obtained for **6d**, and 58% yield was observed for **6n**. Undoubtedly, the yield increased significantly with the decrease in the electronic density of the 1,3-enynes. The method was further applied in the synthesis of chiral spiro compounds. Remarkably, four chiral spiro pyrrolidines were prepared in uniformly high yields and high

enantioselectivity (**7a**, **7d**, **7i**, and **7r**, 80–94%, 89–93% ee). However, the diastereoselectivity was moderate (6/1–14/1 dr). The absolute configuration of **7i** was established by X-ray crystallographic analysis of its single crystals. The stereochemistry of other products (**6** and **7**) was assigned analogically.

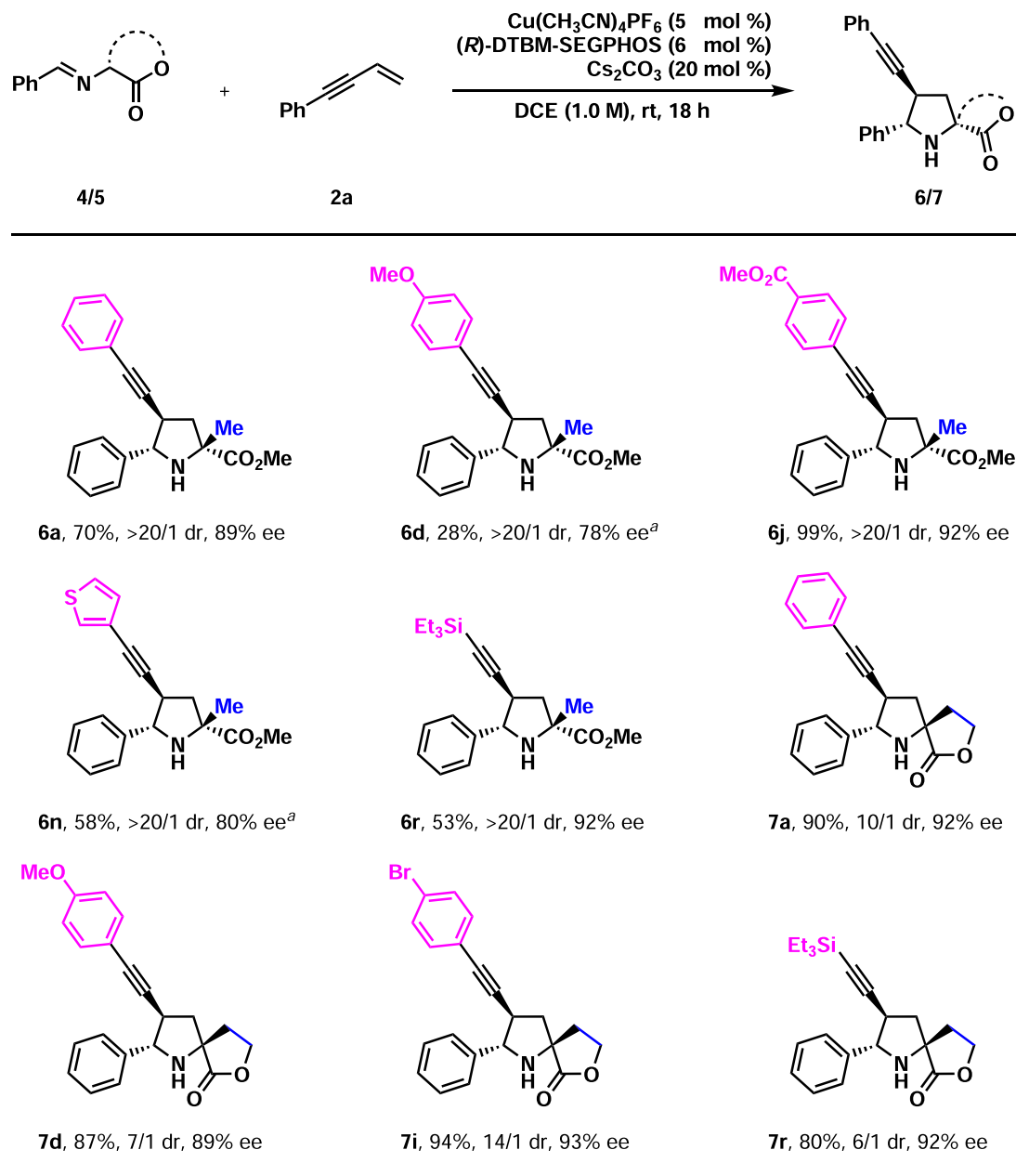


Fig. 5 | Preliminary investigation of the catalytic asymmetric construction of tetrasubstituted carbon. Reaction conditions: **4/5** (0.26 mmol), **2** (0.20 mmol). Isolated yields were reported. Ee and dr were determined by chiral-stationary-phase HPLC analysis. ^a60 °C.

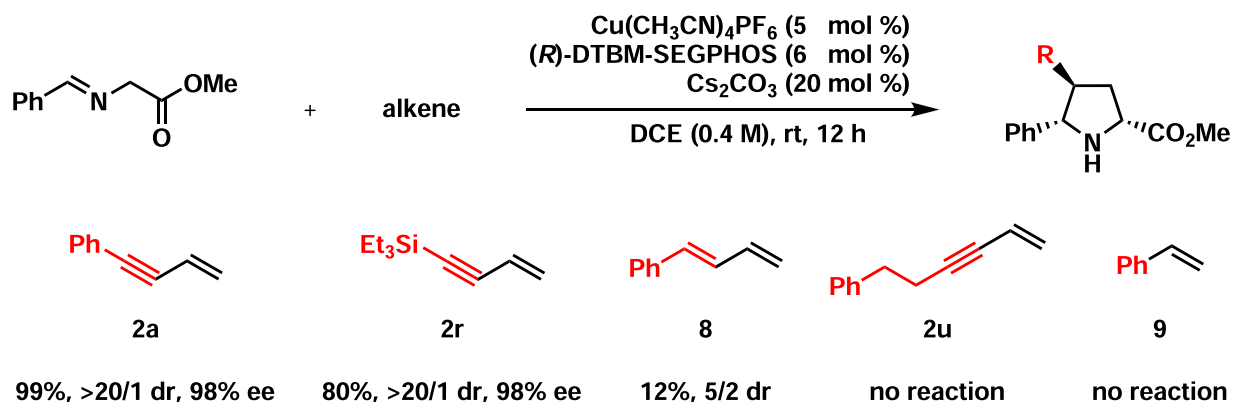


Fig. 6 | Cu(I)-catalyzed asymmetric 1,3-dipolar cycloadditions with several alkenes. Reaction conditions: **1a** (0.26 mmol), alkene (0.20 mmol). Isolated yields were reported. Ee and dr were determined by chiral-stationary-phase HPLC analysis.

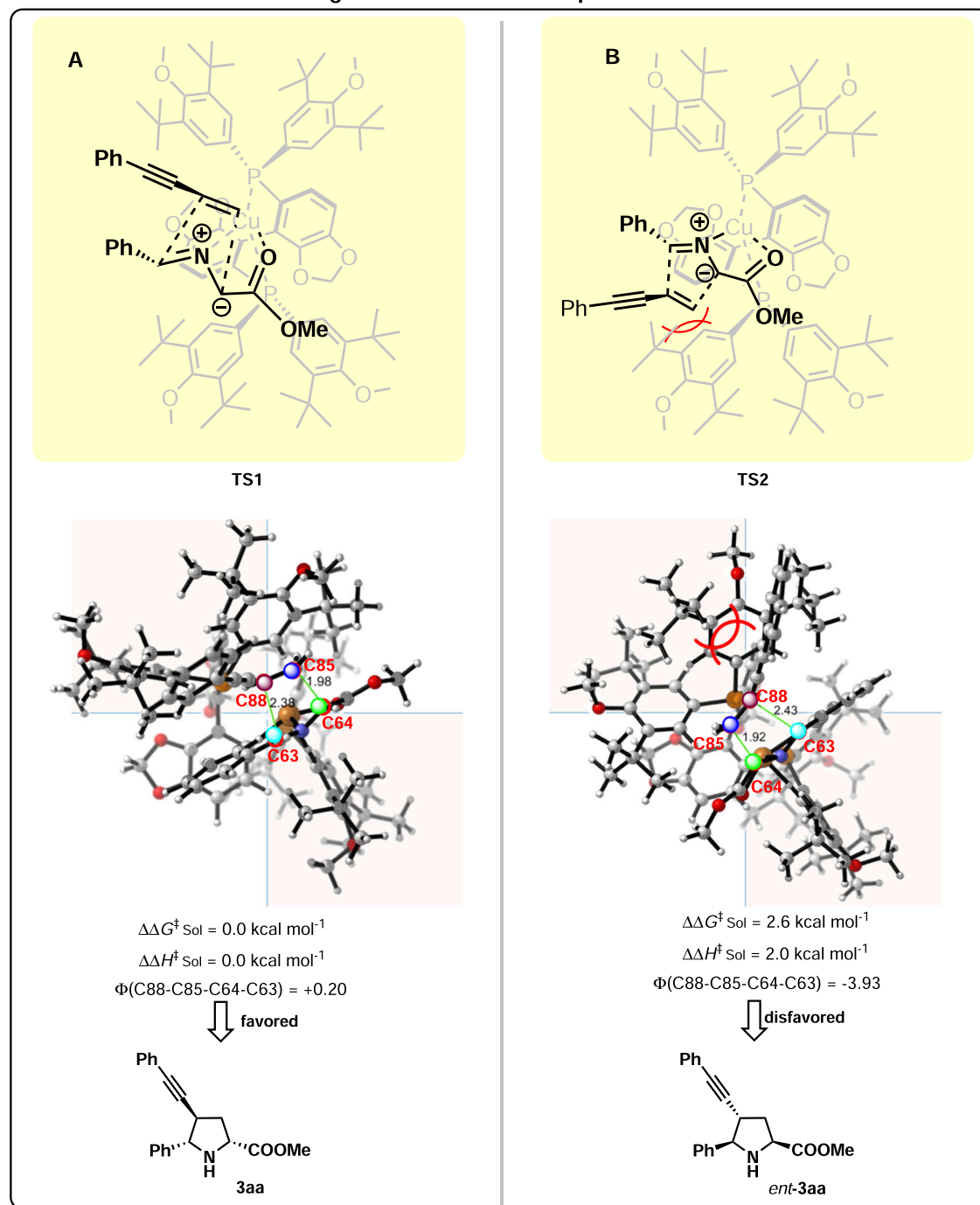
generation of chiral *exo*-products

Fig. 7 | DFT Calculation results: generation of chiral *exo*-products. A Generation of **3aa**. **B** Generation of *ent*-**3aa**.

With the present copper(I)-catalyzed asymmetric 1,3-dipolar cycloaddition as a tool, several olefins, including but-3-en-1-yn-1-ylbenzene (**2a**), but-3-en-1-yn-1-yltriethylsilane (**2r**), (*E*)-buta-1,3-dien-1-ylbenzene (**8**), hex-5-en-3-yn-1-ylbenzene (**2u**), and styrene (**9**), were evaluated. As shown in Fig. 6, **2a** exhibited the highest reactivity, possibly due to the double activation of the olefin by both the conjugated alkyne and the conjugated phenyl groups. **2r** displayed the second-highest reactivity as both the conjugated alkyne group and the triethylsilyl group activated the olefin. Clearly, the phenyl group had a stronger activation effect on the conjugated terminal olefin than the triethylsilyl group. The reaction with **8** was very slow and led to a low yield (12%), indicating that the activation effect of the conjugated

alkene group on the terminal olefin is much weaker than the conjugated alkyne group. Such an experimental fact could be rationalized by the realization that two π -bonds are present in the alkyne while only one π -bond is present in the alkene, which leads to superior activation of the terminal olefin in **2a** to the one in **8**. **2u** and **9** remained intact, suggesting that the activation of the olefin singly by the alkyne or the phenyl is not enough for the present 1,3-dipolar cycloaddition.

In literature³⁶, it was proposed that the copper(I)-catalyzed 1,3-dipolar cycloaddition of strongly activated olefins prefers a stepwise mechanism while the reaction of weakly activated olefins prefers a concerted mechanism. Thus it is believed that the present reaction proceeds preferentially in a concerted mechanism. To elucidate the

mechanistic details, DFT calculations were performed by employing iminoester **1a**, 1,3-enyne **2a**, ligand (*R*)-DTBM-SEGPHOS, and $\text{Cu}(\text{CH}_3\text{CN})_4\text{PF}_6$ as depicted in Fig. 7. The computational results showed that the present reaction proceeded preferentially in a concerted mechanism rather than the stepwise mechanism (for details, see SI). Based on the concerted mechanism, the stereoselectivity-determining cyclization step was revealed, and the relative free energies of the enantio-isomeric transition states and their structures were obtained, which are depicted in Fig. 7. **TS1** (leading to the desired product **3aa**) is more favorable by $2.6 \text{ kcal mol}^{-1}$ than **TS2** (leading to *ent*-**3aa**). Evidently, the calculation results are in good agreement with the experimental enantioselectivity (98% ee), which validates the calculated concerted reaction pathway. Through analysis of the structures of the competing transition states **TS1** and **TS2**, the close distance between one of the *t*Bu groups in (*R*)-DTBM-SEGPHOS and the alkynyl and phenyl groups in 1,3-enyne **2a** in the disfavored **TS2** leads to more van der Waals interactions (for details, see SI) and bigger dihedral angle of C88–C85–C64–C63 in the relatively unfavored cyclization transition state, which results in the observed absolute stereochemistry.

At last, transformations were performed with **3ar** as a model substrate (Fig. 8). The catalytic hydrogenation of **3ar** at room temperature provided silane **10** in 87% yield. The deprotection of **3ar** afforded terminal alkyne **11** in 94% yield. The Sonogashira coupling of **11** with vinylbromide furnished 1,3-enyne **12** in 91% yield. Notably, the coupling proceeded smoothly in the presence of a free secondary

amine moiety. Moreover, the click reaction of **11** and benzyl azide occurred nicely to deliver triazole **13** in 71% yield. The protection of the secondary amine moiety underwent easily gave terminal alkyne **14**, which was ready for the CuI-catalyzed cross-coupling reaction between terminal alkyne and allyl bromide⁷⁴. 1,4-Enyne **15** was synthesized in 90% yield. The hydroboration of the terminal olefin in **15** was readily performed to offer boronate **16** in 60% yield. It should be mentioned that further transformations based on silane, 1,3-enyne, terminal alkyne, terminal olefin, and boronate were straightforward. Moreover, some of the above transformations compensated for the inertness of 4-alkyl-1,3-enynes in the present 1,3-dipolar cycloaddition.

Methods

General procedures for copper(I)-catalyzed asymmetric 1,3-dipolar cycloaddition of 1,3-enynes: a dried 25 ml schlenk tube equipped with a magnetic stirring bar was charged with $[\text{Cu}(\text{MeCN})_4]\text{PF}_6$ (3.7 mg, 0.01 mmol, 0.05 equiv), Cs_2CO_3 (13.0 mg, 0.04 mmol, 0.2 equiv), and (*R*)-DTBM-SEGPHOS (14.0 mg, 0.012 mmol, 0.06 equiv) in a glove box under Ar atmosphere. Anhydrous DCE (0.5 ml) was added via a syringe. The mixture was stirred for 30 min at room temperature. Then imine esters (0.26 mmol, 1.3 equiv) and 1,3-enynes (0.2 mmol, 1.0 equiv) were added sequentially. The resulting mixture was stirred at room temperature for 12 or 18 h. Then the reaction mixture was directly purified by silica gel column chromatography to give the desired product.

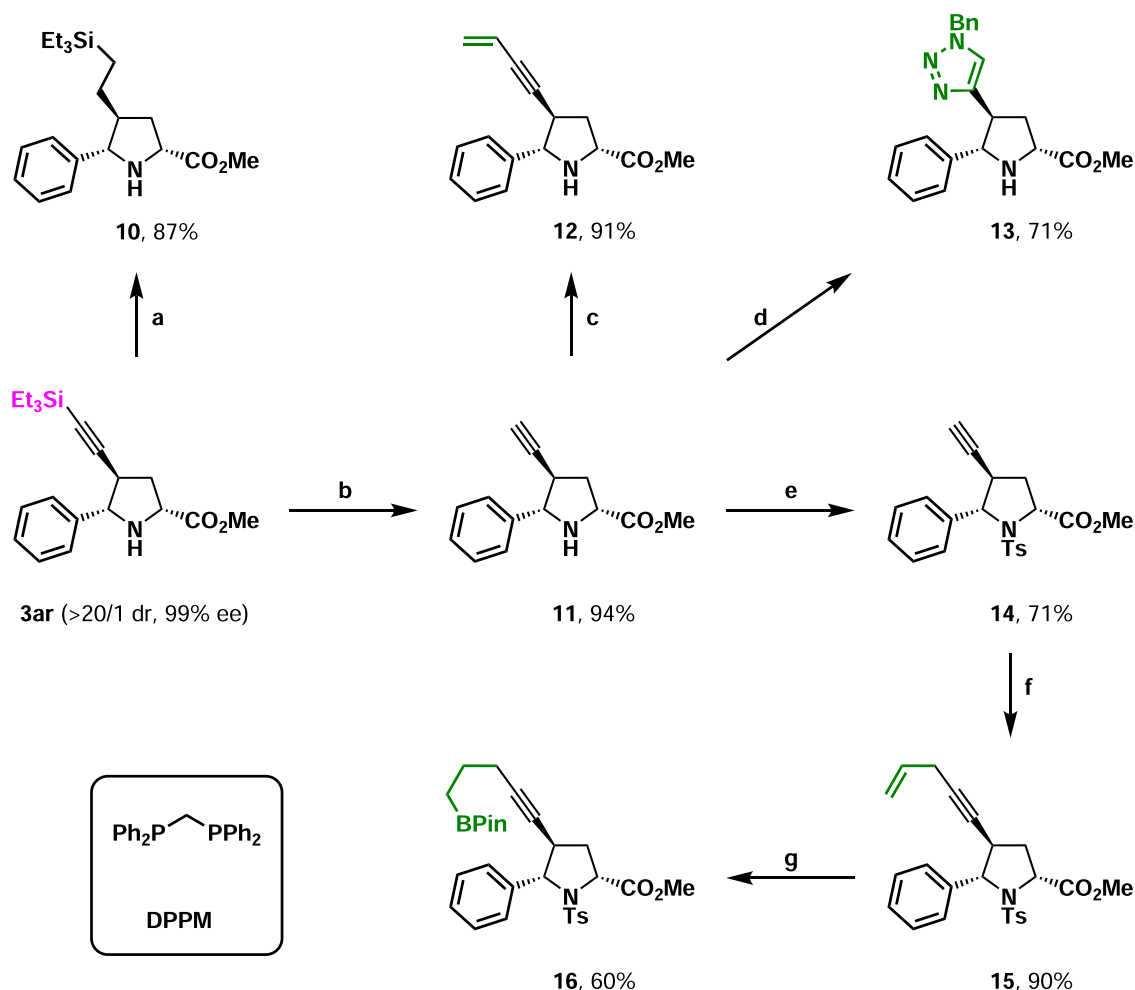


Fig. 8 | Transformations of product **3p**. **a** Reduction. Pd/C, H_2 (1 atm), MeOH, rt. **b** Desilylation. TBAF, THF, 0 °C. **c** Cross-coupling. Vinylbromide, Pd(PPh_3) $_2\text{Cl}_2$, CuI, PPh_3 , NEt_3 , THF, 50 °C. **d** Click reaction. BnN_3 , NaAsc, CuSO_4 , $\text{H}_2\text{O}/\text{DMF}$, 40 °C.

e Protection. TsCl, Et_3N , DMAP, DCM, 0 °C to rt. **f** Cross-coupling. Allylbromide, CuI, TBAI, K_2CO_3 , DMF, rt. **g** Ir-catalyzed hydroboration. $[\text{Ir}(\text{COD})_2\text{Cl}_2]_2$, DPPM, HBPIn, DCM, rt.

Data availability

All data are available from the authors upon request. Supplementary information and chemical compound information are available along with the online version of the paper. The X-ray crystallographic coordinates for structures reported in this study have been deposited at the Cambridge Crystallographic Data Centre (CCDC) under deposition numbers 2093924, 2111662, 2106096, and 2111496. These data can be obtained free of charge from The Cambridge Crystallographic Data Centre via www.ccdc.cam.ac.uk/data_request/cif. Cartesian coordinates of the optimized structures are provided in a supplementary data file.

References

- Ding, K. et al. Structure-based design of potent non-peptide MDM2 inhibitors. *J. Am. Chem. Soc.* **127**, 10130–10131 (2005).
- Michael, J. P. Indolizidine and quinolizidine alkaloids. *Nat. Prod. Rep.* **25**, 139–165 (2008).
- Roughley, S. D. & Jordan, A. M. The medicinal chemist's toolbox: an analysis of reactions used in the pursuit of drug candidates. *J. Med. Chem.* **54**, 3451–3479 (2011).
- Zhao, Y. et al. Diastereomeric spirooxindoles as highly potent and efficacious MDM2 inhibitors. *J. Am. Chem. Soc.* **135**, 7223–7234 (2013).
- Setoguchi, M. et al. A novel, potent, and orally active VLA-4 antagonist with good aqueous solubility: trans-4-[1-[[2-(5-Fluoro-2-methylphenylamino)-7-fluoro-6-benzoxazolyl]acetyl]- (5S)-[methoxy(methyl)amino]methyl-(2S)-pyrrolidinylmethoxy]cyclohexanecarboxylic acid. *Bioorg. Med. Chem.* **21**, 42–61 (2013).
- Zhao, Y., Aguilar, A., Bernard, D. & Wang, S. Small-molecule inhibitors of the MDM2–p53 protein–protein interaction (MDM2 inhibitors) in clinical trials for cancer treatment. *J. Med. Chem.* **58**, 1038–1052 (2015).
- Kuhnert, M., Blum, A., Steuber, H. & Diederich, W. E. Privileged structures meet human T-cell leukemia virus-1 (HTLV-1): C2-symmetric 3,4-disubstituted pyrrolidines as nonpeptidic HTLV-1 protease inhibitors. *J. Med. Chem.* **58**, 4845–4850 (2015).
- Shu, L., Gu, C., Fishlock, D. & Li, Z. Practical synthesis of MDM2 antagonist RG7388. part 1: a Cu(II)-catalyzed asymmetric [3 + 2] cycloaddition. *Org. Process Res. Dev.* **20**, 2050–2056 (2016).
- Scanio, M. J. C. et al. Discovery of ABBV/GLPG-3221, a potent corrector of CFTR for the treatment of cystic fibrosis. *ACS Med. Chem. Lett.* **10**, 1543–1548 (2019).
- Hartung, J., Greszler, S. N., Klis, R. C. & Kallemeyn, J. M. Development of an enantioselective [3 + 2] cycloaddition to synthesize the pyrrolidine core of ABBV-3221 on multikilogram scale. *Org. Process Res. Dev.* **23**, 2532–2537 (2019).
- Pandey, G., Banerjee, P. & Gadre, S. R. Construction of enantiopure pyrrolidine ring system via asymmetric [3+2]-cycloaddition of azomethine ylides. *Chem. Rev.* **106**, 4484–4517 (2006).
- Adrio, J. & Carretero, J. C. Novel dipolarophiles and dipoles in the metal-catalyzed enantioselective 1,3-dipolar cycloaddition of azomethine ylides. *Chem. Commun.* **47**, 6784–6794 (2011).
- Adrio, J. & Carretero, J. C. Recent advances in the catalytic asymmetric 1,3-dipolar cycloaddition of azomethine ylides. *Chem. Commun.* **50**, 12434–12446 (2014).
- Nájera, C. & Sansano, J. M. Coinage metal complexes as chiral catalysts for 1,3-dipolar cycloadditions. *J. Organomet. Chem.* **771**, 78–92 (2014).
- Hashimoto, T. & Maruoka, K. Recent advances of catalytic asymmetric 1,3-dipolar cycloadditions. *Chem. Rev.* **115**, 5366–5412 (2015).
- Fang, X. & Wang, C.-J. Catalytic asymmetric construction of spiropyrrolidines via 1,3-dipolar cycloaddition of azomethine ylides. *Org. Biomol. Chem.* **16**, 2591–2601 (2018).
- Adrio, J. & Carretero, J. C. Stereochemical diversity in pyrrolidine synthesis by catalytic asymmetric 1,3-dipolar cycloaddition of azomethine ylides. *Chem. Commun.* **55**, 11979–11991 (2019).
- Wei, L., Chang, X. & Wang, C.-J. Catalytic asymmetric reactions with N-metallated azomethine ylides. *Acc. Chem. Res.* **53**, 1084–1100 (2020).
- Stanley, L. M. & Sibi, M. P. Enantioselective copper-catalyzed 1,3-dipolar cycloadditions. *Chem. Rev.* **108**, 2887–2902 (2008).
- Fang, X., Zhang, J.-W. & Wang, C.-J. Asymmetric cycloaddition and cascade addition-cyclization reactions. *Top. Organomet. Chem.* **58**, 183–206 (2016).
- Xiong, Y. et al. Well-designed phosphine–urea ligand for highly diastereo- and enantioselective 1,3-dipolar cycloaddition of methacrylonitrile: a combined experimental and theoretical study. *J. Am. Chem. Soc.* **141**, 961–971 (2019).
- Cheng, F. et al. Diastereodivergent asymmetric 1,3-dipolar cycloaddition of azomethine ylides and β -fluoroalkyl vinylsulfones: low copper(II) catalyst loading and theoretical studies. *Angew. Chem. Int. Ed.* **58**, 16637–16643 (2019).
- Chang, X. et al. Copper(I)-catalyzed kinetic resolution of exo-3-oxodicyclopentadienes and endo-3-oxodicyclopentadiene. *Org. Lett.* **21**, 1191–1196 (2019).
- Gan, Z. et al. P-stereogenic phosphines directed copper(I)-catalyzed enantioselective 1,3-dipolar cycloadditions. *Org. Lett.* **21**, 2782–2785 (2019).
- Liang, L. et al. Facile synthesis of chiral [2,3]-fused hydrobenzofuran via asymmetric Cu(I)-catalyzed dearomative 1,3-dipolar cycloaddition. *Chem. Commun.* **55**, 553–556 (2019).
- Deng, H., Jia, R., Yang, W.-L., Yu, X. & Deng, W.-P. Ligand-controlled switch in diastereoselectivities: catalytic asymmetric construction of spirocyclic pyrrolidine-azetidine/oxe(thie)tane derivatives. *Chem. Commun.* **55**, 7346–7349 (2019).
- Liu, B., Li, W., Wu, H.-H. & Zhang, J. Enantiodivergent synthesis of 1,2-bis(diphenylphosphino)ethanes via asymmetric [3 + 2]-cycloaddition. *Org. Chem. Front.* **6**, 694–698 (2019).
- Caleffi, G. S. et al. Switching diastereoselectivity in catalytic enantioselective (3+2) cycloadditions of azomethine ylides promoted by metal salts and privileged sephos-derived ligands. *J. Org. Chem.* **84**, 10593–10605 (2019).
- Shen, C. et al. Kinetic resolution of alkylidene norcamphors via a ligand-controlled umpolung-type 1,3-dipolar cycloaddition. *iScience* **11**, 146–159 (2019).
- Furuya, S., Kato, S., Kanemoto, K. & Fukuzawa, S. Copper-catalyzed regio- and diastereoselective 1,3-dipolar cycloaddition reactions of glycine imino esters with 1-propene-1,3-sultone. *Eur. J. Org. Chem.* **2019**, 4561–4565 (2019).
- Wang, Z., Wang, D.-C. & Xie, M.-S. Enantioselective synthesis of fused polycyclic tropanes via dearomative [3 + 2] cycloaddition reactions of 2-nitrobenzofurans. *Org. Lett.* **22**, 164–167 (2020).
- Cui, H. et al. Copper(I)/Ganphos catalysis: enantioselective synthesis of diverse spirooxindoles using iminoesters and alkyl substituted methyleneindolinones. *Org. Biomol. Chem.* **18**, 3740–3746 (2020).
- Cheng, X., Yan, D., Dong, X.-Q. & Wang, C.-J. Chiral tri-fluoromethylated pyrrolidines via Cu-catalyzed asymmetric 1,3-dipolar cycloaddition. *Asian J. Org. Chem.* **9**, 1567–1570 (2020).
- Li, Y.-N., Chang, X., Xiong, Q., Dong, X.-Q. & Wang, C.-J. Cu-catalyzed endo-selective asymmetric 1,3-dipolar cycloaddition of azomethine ylides with ethenesulfonyl fluorides: efficient access to chiral pyrrolidine-3-sulfonyl fluorides. *Chinese Chem. Lett.* <https://doi.org/10.1016/j.ccl.2021.05.063> (2021).
- González-Esguevillas, M., Pascual-Escudero, A., Adrio, J. & Carretero, J. C. Highly selective copper-catalyzed asymmetric [3 + 2]

- cycloaddition of azomethine ylides with acyclic 1,3-dienes. *Chem. Eur. J.* **21**, 4561–4565 (2015).
36. Pascual-Escudero, A., Cózar, A. D., Cossio, F. P., Adrio, J. & Carretero, J. C. Alkenyl arenes as dipolarophiles in catalytic asymmetric 1,3-dipolar cycloaddition reactions of azomethine ylides. *Angew. Chem. Int. Ed.* **55**, 15334–15338 (2016).
37. Liu, K., Xiong, Y., Wang, Z.-F., Tao, H.-Y. & Wang, C.-J. Ligand-controlled stereodivergent 1,3-dipolar cycloaddition of azomethine ylides with 3-methyl-4-nitro-5-styrylisoxazoles. *Chem. Commun.* **52**, 9458–9461 (2016).
38. Chang, X. et al. β -Substituted alkenyl heteroarenes as dipolarophiles in the Cu(I)-catalyzed asymmetric 1,3-dipolar cycloaddition of azomethine ylides empowered by a dual activation strategy: stereoselectivity and mechanistic insight. *J. Am. Chem. Soc.* **143**, 3519–3535 (2021).
39. Filippone, S., Maroto, E. E., Martín-Domenech, Á., Suarez, M. & Martín, N. An efficient approach to chiral fullerene derivatives by catalytic enantioselective 1,3-dipolar cycloadditions. *Nat. Chem.* **1**, 578–582 (2009).
40. Maroto, E. E., Filippone, S., Martín-Domenech, A., Suarez, M. & Martín, N. Switching the stereoselectivity: (fullero)pyrrolidines “a la carte”. *J. Am. Chem. Soc.* **134**, 12936–12938 (2012).
41. Maroto, E. E. et al. Chiral fullerenes from asymmetric catalysis. *Acc. Chem. Res.* **47**, 2660–2670 (2014).
42. Filatov, A. S. et al. A highly diastereoselective one-pot three-component 1,3-dipolar cycloaddition of cyclopropenes with azomethine ylides generated from 11*H*-indeno[1,2-*b*]-quinoxalin-11-ones. *Org. Chem. Front.* **5**, 595–605 (2018).
43. Deng, H., Yang, W.-L., Tian, F., Tang, W. & Deng, W.-P. Asymmetric construction of 3-azabicyclo[3.1.0]hexane skeleton with five contiguous stereogenic centers by Cu-catalyzed 1,3-dipolar cycloaddition of trisubstituted cyclopropenes. *Org. Lett.* **20**, 4121–4125 (2018).
44. Saito, S. & Yamamoto, Y. Recent advances in the transition-metal-catalyzed regioselective approaches to polysubstituted benzene derivatives. *Chem. Rev.* **100**, 2901–2915 (2000).
45. Wessig, P. & Müller, G. The dehydro-Diels–Alder reaction. *Chem. Rev.* **108**, 205m1–2063m1 (2008).
46. Jang, H.-Y., Huddleston, R. R. & Krische, M. J. Hydrogen-mediated C–C bond formation: catalytic regio- and stereoselective reductive condensation of α -keto aldehydes and 1,3-enynes. *J. Am. Chem. Soc.* **126**, 4664–4668 (2004).
47. Kong, J.-R., Cho, C.-W. & Krische, M. J. Hydrogen-mediated reductive coupling of conjugated alkynes with ethyl (N-sulfinyl)iminoacetates: synthesis of unnatural α -amino acids via rhodium-catalyzed C–C bond forming hydrogenation. *J. Am. Chem. Soc.* **127**, 11269–11276 (2005).
48. Kong, J.-R., Ngai, M.-Y. & Krische, M. J. Highly enantioselective direct reductive coupling of conjugated alkynes and α -ketoesters via rhodium-catalyzed asymmetric hydrogenation. *J. Am. Chem. Soc.* **128**, 718–719 (2006).
49. Komanduri, V. & Krische, M. J. Enantioselective reductive coupling of 1,3-enynes to heterocyclic aromatic aldehydes and ketones via rhodium-catalyzed asymmetric hydrogenation: mechanistic insight into the role of Brønsted acid additives. *J. Am. Chem. Soc.* **128**, 16448–16449 (2006).
50. Cho, C.-W. & Krische, M. J. Enantioselective reductive coupling of alkynes and α -keto aldehydes via rhodium-catalyzed hydrogenation: an approach to bryostatin substructures. *Org. Lett.* **8**, 891–894 (2006).
51. Hong, Y.-T., Cho, C.-W., Skucas, E. & Krische, M. J. Enantioselective reductive coupling of 1,3-enynes to glyoxalates mediated by hydrogen: asymmetric synthesis of β,γ -unsaturated α -hydroxy esters. *Org. Lett.* **9**, 3745–3748 (2007).
52. Patman, R. L., Williams, V. M., Bower, J. F. & Krische, M. J. Carbonyl propargylation from the alcohol or aldehyde oxidation level employing 1,3-enynes as surrogates to preformed allenylmetal reagents: a ruthenium-catalyzed C–C bond-forming transfer hydrogenation. *Angew. Chem. Int. Ed.* **47**, 5220–5223 (2008).
53. Geary, L. M., Woo, S. K., Leung, J. C. & Krische, M. J. Diastereo- and enantioselective iridium-catalyzed carbonyl propargylation from the alcohol or aldehyde oxidation level: 1,3-enynes as allenylmetal equivalents. *Angew. Chem. Int. Ed.* **51**, 2972–2976 (2012).
54. Geary, L. M., Leung, J. C. & Krische, M. J. Ruthenium-catalyzed reductive coupling of 1,3-enynes and aldehydes by transfer hydrogenation: anti-diastereoselective carbonyl propargylation. *Chem. Eur. J.* **18**, 16823–16827 (2012).
55. Nguyen, K. D., Herkommer, D. & Krische, M. J. Ruthenium-BINAP catalyzed alcohol C–H tert-prenylation via 1,3-enyne transfer hydrogenation: beyond stoichiometric carbanions in enantioselective carbonyl propargylation. *J. Am. Chem. Soc.* **138**, 5238–5241 (2016).
56. Holmes, M., Schwartz, L. A. & Krische, M. J. Intermolecular metal-catalyzed reductive coupling of dienes, allenes, and enynes with carbonyl compounds and imines. *Chem. Rev.* **118**, 6026–6052 (2018).
57. Fu, L., Greßies, S., Chen, P. & Liu, G. Recent advances and perspectives in transition metal-catalyzed 1,4-functionalizations of unactivated 1,3-enynes for the synthesis of allenes. *Chin. J. Chem.* **38**, 91–100 (2020).
58. Dherbassy, Q. et al. Copper-catalyzed functionalization of enynes. *Chem. Sci.* **11**, 11380–11393 (2020).
59. Meng, F., Haefner, F. & Hoveyda, A. H. Diastereo- and enantioselective reactions of bis(pinacolato)diboron, 1,3-enynes, and aldehydes catalyzed by an easily accessible bisphosphine–Cu complex. *J. Am. Chem. Soc.* **136**, 11304–11307 (2014).
60. Yang, Y., Perry, I. B., Lu, G., Liu, P. & Buchwald, S. L. Copper-catalyzed asymmetric addition of olefin-derived nucleophiles to ketones. *Science* **353**, 144–150 (2016).
61. Gan, X.-C., Zhang, Q., Jia, X.-S. & Yin, L. Asymmetric construction of fluoroalkyl tertiary alcohols through a three-component reaction of (Bpin)₂, 1,3-enynes, and fluoroalkyl ketones catalyzed by a copper(I) complex. *Org. Lett.* **20**, 1070–1073 (2018).
62. Gan, X.-C. & Yin, L. Asymmetric borylative propargylation of ketones catalyzed by a copper(I) complex. *Org. Lett.* **21**, 931–936 (2019).
63. Manna, S., Dherbassy, Q., Perry, G. J. P. & Procter, D. J. Enantio- and diastereoselective synthesis of homopropargyl amines by copper-catalyzed coupling of imines, 1,3-enynes, and diborons. *Angew. Chem. Int. Ed.* **59**, 4879–4882 (2020).
64. Huang, Y., del Pozo, J., Torker, S. & Hoveyda, A. H. Enantioselective synthesis of trisubstituted allenyl–B(pin) compounds by phosphine–Cu-catalyzed 1,3-enyne hydroboration. insights regarding stereochemical integrity of Cu–allenyl intermediates. *J. Am. Chem. Soc.* **140**, 2643–2655 (2018).
65. Gao, D.-W. et al. Catalytic, enantioselective synthesis of allenyl boronates. *ACS Catal.* **8**, 3650–3654 (2018).
66. Sang, H. J., Yu, S. & Ge, S. Copper-catalyzed asymmetric hydroboration of 1,3-enynes with pinacolborane to access chiral allenylboronates. *Org. Chem. Front.* **5**, 1284–1287 (2018).
67. Yu, S., Sang, H. L., Zhang, S.-Q., Hong, X. & Ge, S. Catalytic asymmetric synthesis of chiral trisubstituted heteroaromatic allenes from 1,3-enynes. *Commun. Chem.* **1**, 64 (2018).
68. Bayeh-Romero, L. & Buchwald, S. L. Copper hydride catalyzed enantioselective synthesis of axially chiral 1,3-disubstituted allenes. *J. Am. Chem. Soc.* **141**, 13788–13794 (2019).
69. Zeng, Y. et al. Copper-catalyzed enantioselective radical 1,4-difunctionalization of 1,3-enynes. *J. Am. Chem. Soc.* **142**, 18014–18021 (2020).
70. Liao, Y. et al. Enantioselective synthesis of multisubstituted allenes by cooperative Cu/Pd-catalyzed 1,4-arylboration of 1,3-enynes. *Angew. Chem. Int. Ed.* **59**, 1176–1180 (2020).

71. He, C.-Y. et al. Copper(I)-catalyzed diastereo- and enantio-selective construction of optically pure exocyclic allenes. *Nat. Commun.* **11**, 4293 (2020).
72. Yang, C. et al. Catalytic asymmetric conjugate protosilylation and protoborylation of 2-trifluoromethyl enynes for synthesis of functionalized allenes. *Org. Lett.* **22**, 1360–1367 (2020).
73. Ye, J. et al. Halogenated salt assisted Cu-catalyzed asymmetric 1,4-borylstannation of 1,3-enynes: enantioselective synthesis of allenylstannanes. *Chem. Sci.* **12**, 3032–3038 (2021).
74. Bumagin, N. A., Ponomarev, A. B. & Beletskaya, I. P. Synthesis of allylacetylenes from terminal acetylenes and allyl halides. *Bull. Acad. Sci. USSR Div. Chem. Sci. (Engl. Transl.)* **36**, 1445–1448 (1987).
75. Yamamoto, Y., Fujikawa, R., Umemoto, T. & Miyaura, N. Iridium-catalyzed hydroboration of alkenes with pinacolborane. *Tetrahedron* **60**, 10695–10700 (2004).

Acknowledgements

We gratefully acknowledge the financial support from the National Natural Science Foundation of China (Nos. 21871287, 21922114, and 22271302), the Science and Technology Commission of Shanghai Municipality (Nos. 20JC1417100, 21XD1424800, and 20400750300), the Innovation Team and Talents Cultivation Program of National Administration of Traditional Chinese Medicine (ZYYCXTD-202004), CAS Key Laboratory of Synthetic Chemistry of Natural Substances, and Shanghai Institute of Organic Chemistry. We are also grateful to Professor Xin Hong and Professor Xiao-Song Xue for their help and advices on the chemical calculations. Moreover, Mr. Jia-Wei Jiang is acknowledged for the check on the reproducibility of this work.

Author contributions

L.Y., P.T., and D.D.G. conceived and designed the study. B.R.W., Y.B.L., and Q.Z. performed the synthetic experiments and analyzed data for all new compounds. Q.H.L. did the chemical calculation work. L.Y. and P.T. wrote the paper.

Competing interests

The authors declare no competing interests.

Additional information

Supplementary information The online version contains supplementary material available at <https://doi.org/10.1038/s41467-023-40409-4>.

Correspondence and requests for materials should be addressed to Ping Tian, Qinghua Li or Liang Yin.

Peer review information *Nature Communications* thanks the anonymous reviewers for their contribution to the peer review of this work.

Reprints and permissions information is available at <http://www.nature.com/reprints>

Publisher's note Springer Nature remains neutral with regard to jurisdictional claims in published maps and institutional affiliations.

Open Access This article is licensed under a Creative Commons Attribution 4.0 International License, which permits use, sharing, adaptation, distribution and reproduction in any medium or format, as long as you give appropriate credit to the original author(s) and the source, provide a link to the Creative Commons license, and indicate if changes were made. The images or other third party material in this article are included in the article's Creative Commons license, unless indicated otherwise in a credit line to the material. If material is not included in the article's Creative Commons license and your intended use is not permitted by statutory regulation or exceeds the permitted use, you will need to obtain permission directly from the copyright holder. To view a copy of this license, visit <http://creativecommons.org/licenses/by/4.0/>.

© The Author(s) 2023